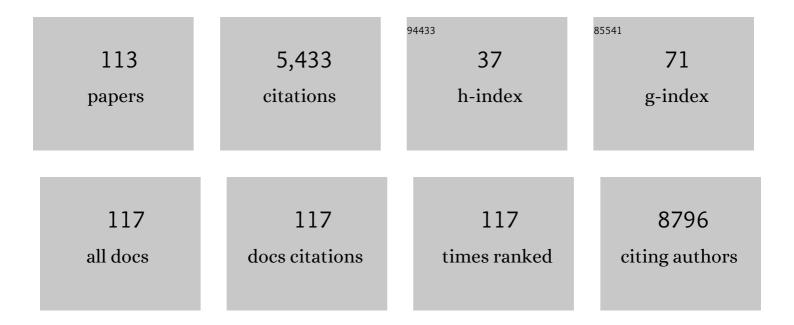
Andres Osvet

List of Publications by Year in descending order

Source: https://exaly.com/author-pdf/1963744/publications.pdf Version: 2024-02-01



....

#	ARTICLE	IF	CHAIIONS
1	Rareâ€Earth Ion Doped Upâ€Conversion Materials for Photovoltaic Applications. Advanced Materials, 2011, 23, 2675-2680.	21.0	465
2	High-performance direct conversion X-ray detectors based on sintered hybrid lead triiodide perovskite wafers. Nature Photonics, 2017, 11, 436-440.	31.4	442
3	Brightly Luminescent and Color-Tunable Formamidinium Lead Halide Perovskite FAPbX ₃ (X) Tj ETQq1	1 0.7843 9.1	14 rgBT /0
4	Giant Rashba Splitting in <mml:math <br="" xmlns:mml="http://www.w3.org/1998/Math/MathML">display="inline"><mml:msub><mml:mi>CH</mml:mi><mml:mn>3</mml:mn></mml:msub><mml:msub><mml:mi Perovskite. Physical Review Letters, 2016, 117, 126401.</mml:mi </mml:msub></mml:math>	> MIs <td>:2769<mml:< td=""></mml:<></td>	:2769 <mml:< td=""></mml:<>
5	The role of exciton lifetime for charge generation in organic solar cells at negligible energy-level offsets. Nature Energy, 2020, 5, 711-719.	39.5	214
6	Overcoming the Interface Losses in Planar Heterojunction Perovskiteâ€Based Solar Cells. Advanced Materials, 2016, 28, 5112-5120.	21.0	188
7	Local Observation of Phase Segregation in Mixed-Halide Perovskite. Nano Letters, 2018, 18, 2172-2178.	9.1	186
8	"Black―TiO ₂ Nanotubes Formed by High-Energy Proton Implantation Show Noble-Metal- <i>co</i> -Catalyst Free Photocatalytic H ₂ -Evolution. Nano Letters, 2015, 15, 6815-6820.	9.1	174
9	Thermal-Driven Phase Separation of Double-Cable Polymers Enables Efficient Single-Component Organic Solar Cells. Joule, 2019, 3, 1765-1781.	24.0	124
10	A bilayer conducting polymer structure for planar perovskite solar cells with over 1,400 hours operational stability at elevated temperatures. Nature Energy, 2022, 7, 144-152.	39.5	123
11	Photoinduced degradation of methylammonium lead triiodide perovskite semiconductors. Journal of Materials Chemistry A, 2016, 4, 15896-15903.	10.3	119
12	Structural fluctuations cause spin-split states in tetragonal (CH ₃ NH ₃)PbI ₃ as evidenced by the circular photogalvanic effect. Proceedings of the National Academy of Sciences of the United States of America, 2018, 115, 9509-9514.	7.1	106
13	Ligand-assisted thickness tailoring of highly luminescent colloidal CH ₃ NH ₃ PbX ₃ (X = Br and I) perovskite nanoplatelets. Chemical Communications, 2017, 53, 244-247.	4.1	99
14	Simultaneous excitation of Ce3+ and Eu3+ ions in Tb3Al5O12. Radiation Measurements, 2004, 38, 539-543.	1.4	98
15	Timeâ€Dependent Morphology Evolution of Solutionâ€Processed Small Molecule Solar Cells during Solvent Vapor Annealing. Advanced Energy Materials, 2016, 6, 1502579.	19.5	96
16	Hydrogenated Anatase: Strong Photocatalytic Dihydrogen Evolution without the Use of a Coâ€Catalyst. Angewandte Chemie - International Edition, 2014, 53, 14201-14205.	13.8	87
17	Strain-activated light-induced halide segregation in mixed-halide perovskite solids. Nature Communications, 2020, 11, 6328.	12.8	86
18	Sensitive Direct Converting Xâ€Ray Detectors Utilizing Crystalline CsPbBr ₃ Perovskite Films Fabricated via Scalable Melt Processing. Advanced Materials Interfaces, 2020, 7, 1901575.	3.7	83

#	Article	IF	CITATIONS
19	Inverted, Environmentally Stable Perovskite Solar Cell with a Novel Lowâ€Cost and Waterâ€Free PEDOT Holeâ€Extraction Layer. Advanced Energy Materials, 2015, 5, 1500543.	19.5	81
20	Discovery of temperature-induced stability reversal in perovskites using high-throughput robotic learning. Nature Communications, 2021, 12, 2191.	12.8	77
21	Exploring the Stability of Novel Wide Bandgap Perovskites by a Robot Based High Throughput Approach. Advanced Energy Materials, 2018, 8, 1701543.	19.5	75
22	Revealing Hidden UV Instabilities in Organic Solar Cells by Correlating Device and Material Stability. Advanced Energy Materials, 2019, 9, 1902124.	19.5	74
23	Effective Ligand Engineering of the Cu ₂ ZnSnS ₄ Nanocrystal Surface for Increasing Hole Transport Efficiency in Perovskite Solar Cells. Advanced Functional Materials, 2016, 26, 8300-8306.	14.9	72
24	Exploring the Limiting Openâ€Circuit Voltage and the Voltage Loss Mechanism in Planar CH ₃ NH ₃ PbBr ₃ Perovskite Solar Cells. Advanced Energy Materials, 2016, 6, 1600132.	19.5	71
25	Robot-Based High-Throughput Screening of Antisolvents for Lead Halide Perovskites. Joule, 2020, 4, 1806-1822.	24.0	65
26	Water Ingress in Encapsulated Inverted Organic Solar Cells: Correlating Infrared Imaging and Photovoltaic Performance. Advanced Energy Materials, 2015, 5, 1501065.	19.5	60
27	Nobleâ€Metalâ€Free Photocatalytic Hydrogen Evolution Activity: The Impact of Ball Milling Anatase Nanopowders with TiH ₂ . Advanced Materials, 2017, 29, 1604747.	21.0	59
28	Effective Ligand Passivation of Cu ₂ O Nanoparticles through Solid-State Treatment with Mercaptopropionic Acid. Journal of the American Chemical Society, 2014, 136, 7233-7236.	13.7	57
29	Suppression of Hysteresis Effects in Organohalide Perovskite Solar Cells. Advanced Materials Interfaces, 2017, 4, 1700007.	3.7	57
30	Synthesis and Spectroscopic Investigations of Cu- and Pb-Doped Colloidal ZnS Nanocrystals. Journal of Physical Chemistry B, 2006, 110, 23175-23178.	2.6	49
31	Extending the environmental lifetime of unpackaged perovskite solar cells through interfacial design. Journal of Materials Chemistry A, 2016, 4, 11604-11610.	10.3	49
32	Overcoming Microstructural Limitations in Water Processed Organic Solar Cells by Engineering Customized Nanoparticulate Inks. Advanced Energy Materials, 2018, 8, 1702857.	19.5	48
33	Assessing Temperature Dependence of Drift Mobility in Methylammonium Lead Iodide Perovskite Single Crystals. Journal of Physical Chemistry C, 2018, 122, 5935-5939.	3.1	47
34	Up-conversion semiconducting MoO3:Yb/Er nanocomposites as buffer layer in organic solar cells. Solar Energy Materials and Solar Cells, 2012, 105, 196-201.	6.2	46
35	Intrinsically Activated SrTiO ₃ : Photocatalytic H ₂ Evolution from Neutral Aqueous Methanol Solution in the Absence of Any Noble Metal Cocatalyst. ACS Applied Materials & Interfaces, 2018, 10, 29532-29542.	8.0	46
36	Printed Smart Photovoltaic Window Integrated with an Energyâ€Saving Thermochromic Layer. Advanced Optical Materials, 2015, 3, 1524-1529.	7.3	43

#	Article	IF	CITATIONS
37	Temperature-dependent optical spectra of single-crystal <mml:math xmlns:mml="http://www.w3.org/1998/Math/MathML"><mml:mo>(</mml:mo><mml:mrow><mml:msub><mml: cleaved in ultrahigh vacuum. Physical Review B, 2017, 95, .</mml: </mml:msub></mml:mrow></mml:math 	mi> £⊎ <td>ml:#roi> < mml</td>	ml:#roi> < mml
38	Nanostructured organosilicon luminophores in highly efficient luminescent down-shifting layers for thin film photovoltaics. Solar Energy Materials and Solar Cells, 2016, 155, 1-8.	6.2	39
39	Visualizing and Suppressing Nonradiative Losses in High Open-Circuit Voltage n-i-p-Type CsPbl ₃ Perovskite Solar Cells. ACS Energy Letters, 2020, 5, 271-279.	17.4	39
40	Understanding the correlation and balance between the miscibility and optoelectronic properties of polymer–fullerene solar cells. Journal of Materials Chemistry A, 2017, 5, 17570-17579.	10.3	35
41	Synthesis and photoluminescent properties of the Dy3+ doped YSO as a high-temperature thermographic phosphor. Journal of Luminescence, 2018, 197, 23-30.	3.1	34
42	Quantum yield of Eu2+ emission in (Ca1â^'xSrx)S:Eu light emitting diode converter at 20–420K. Radiation Measurements, 2010, 45, 350-352.	1.4	32
43	Deciphering the Role of Impurities in Methylammonium Iodide and Their Impact on the Performance of Perovskite Solar Cells. Advanced Materials Interfaces, 2016, 3, 1600593.	3.7	31
44	High-temperature thermographic phosphor mixture YAP/YAG:Dy3+ and its photoluminescence properties. Journal of Luminescence, 2017, 188, 582-588.	3.1	31
45	Real-time evaluation of thin film drying kinetics using an advanced, multi-probe optical setup. Journal of Materials Chemistry C, 2016, 4, 2178-2186.	5.5	29
46	Qualitative Analysis of Bulk-Heterojunction Solar Cells without Device Fabrication: An Elegant and Contactless Method. Journal of the American Chemical Society, 2014, 136, 10949-10955.	13.7	28
47	Suppression of Thermally Induced Fullerene Aggregation in Polyfullerene-Based Multiacceptor Organic Solar Cells. ACS Applied Materials & amp; Interfaces, 2017, 9, 10971-10982.	8.0	26
48	Intercalating-Organic-Cation-Induced Stability Bowing in Quasi-2D Metal-Halide Perovskites. ACS Energy Letters, 2022, 7, 70-77.	17.4	26
49	On the energy transfer from Tb3+ to Eu3+ in LiTb1â^'xEuxP4O12. Radiation Measurements, 2004, 38, 529-532.	1.4	25
50	Polymer-assisted sol–gel process for the preparation of photostimulable core/shell structured SiO 2 Zn 2 SiO 4 :Mn 2+ particles. Materials Chemistry and Physics, 2014, 148, 1055-1063.	4.0	23
51	Controlling additive behavior to reveal an alternative morphology formation mechanism in polymer : fullerene bulk-heterojunctions. Journal of Materials Chemistry A, 2016, 4, 16136-16147.	10.3	22
52	Time-Resolved Analysis of Dielectric Mirrors for Vapor Sensing. ACS Applied Materials & Interfaces, 2018, 10, 36398-36406.	8.0	21
53	Epitaxial Metal Halide Perovskites by Inkjetâ€Printing on Various Substrates. Advanced Functional Materials, 2020, 30, 2004612.	14.9	21
54	A Cross‣inked Interconnecting Layer Enabling Reliable and Reproducible Solutionâ€Processing of Organic Tandem Solar Cells. Advanced Energy Materials, 2020, 10, 1903800.	19.5	21

#	Article	IF	CITATIONS
55	Synthesis, crystal structures and luminescence properties of the Eu3+-doped yttrium oxotellurates(IV) Y2Te4O11 and Y2Te5O13. Journal of Solid State Chemistry, 2008, 181, 2783-2788.	2.9	20
56	Single molecular precursor ink for AgBiS ₂ thin films: synthesis and characterization. Journal of Materials Chemistry C, 2018, 6, 7642-7651.	5.5	20
57	Photoluminescence properties of thermographic phosphors YAG:Dy and YAG:Dy, Er doped with boron and nitrogen. Applied Physics B: Lasers and Optics, 2016, 122, 1.	2.2	19
58	Enhanced photosynthetic activity in Spinacia oleracea by spectral modification with a photoluminescent light converting material. Optics Express, 2013, 21, A909.	3.4	18
59	Increased thermal stabilization of polymer photovoltaic cells with oligomeric PCBM. Journal of Materials Chemistry C, 2016, 4, 8121-8129.	5.5	18
60	Optimization of Solutionâ€Processed Luminescent Downâ€6hifting Layers for Photovoltaics by Customizing Organic Dye Based Thick Films. Energy Technology, 2016, 4, 385-392.	3.8	16
61	Noble metal free photocatalytic H2 generation on black TiO2: On the influence of crystal facets vs. crystal damage. Applied Physics Letters, 2017, 110, .	3.3	16
62	New silicate based thermographic phosphors Ca3Sc2Si3O12:Dy, Ca3Sc2Si3O12:Dy,Ce and their photoluminescence properties. Journal of Luminescence, 2018, 202, 13-19.	3.1	16
63	Assembling Mesoscale‧tructured Organic Interfaces in Perovskite Photovoltaics. Advanced Materials, 2019, 31, e1806516.	21.0	16
64	Looking beyond the Surface: The Band Gap of Bulk Methylammonium Lead Iodide. Nano Letters, 2020, 20, 3090-3097.	9.1	16
65	Unraveling the Chargeâ€Carrier Dynamics from the Femtosecond to the Microsecond Time Scale in Doubleâ€Cable Polymerâ€Based Singleâ€Component Organic Solar Cells. Advanced Energy Materials, 2022, 12, 2103406.	19.5	15
66	Synthesis and optical properties of luminescent core–shell structured silicate and phosphate nanoparticles. Optical Materials, 2011, 33, 1106-1110.	3.6	14
67	Luminescent silicate core–shell nanoparticles: Synthesis, functionalization, optical, and structural properties. Journal of Colloid and Interface Science, 2011, 358, 32-38.	9.4	14
68	Sub-bandgap photon harvesting for organic solar cells via integrating up-conversion nanophosphors. Organic Electronics, 2015, 19, 113-119.	2.6	13
69	Improved charge carrier dynamics in polymer/perovskite nanocrystal based hybrid ternary solar cells. Physical Chemistry Chemical Physics, 2018, 20, 23674-23683.	2.8	13
70	High-Throughput Time-Resolved Photoluminescence Study of Composition- and Size-Selected Aqueous Ag–In–S Quantum Dots. Journal of Physical Chemistry C, 2021, 125, 12185-12197.	3.1	13
71	"Green―synthesis of highly luminescent lead-free Cs ₂ Ag _{<i>x</i>} Na _{1â^'<i>x</i>} Bi _{<i>y</i>} In _{1â^'<i>y</i> perovskites. Journal of Materials Chemistry C, 2022, 10, 9938-9944.}	/s 5⊾5 >Cl≺s	ս և։։ 6
72	(Gd,Lu)AlO ₃ :Dy ³⁺ and (Gd,Lu) ₃ Al ₅ O ₁₂ :Dy ³⁺ as high-temperature thermographic phosphors. Measurement Science and Technology, 2019, 30, 034001.	2.6	12

#	Article	IF	CITATIONS
73	Micro-powder Ca3Sc2Si3O12:Ce silicate garnets as efficient light converters for WLEDs. Optical Materials, 2020, 107, 109978.	3.6	12
74	Highâ€Throughput Robotic Synthesis and Photoluminescence Characterization of Aqueous Multinary Copper–Silver Indium Chalcogenide Quantum Dots. Particle and Particle Systems Characterization, 2021, 38, 2100169.	2.3	12
75	A New Crystal Phase Molybdate Yb ₂ Mo ₄ O ₁₅ : The Synthesis and Upconversion Properties. Particle and Particle Systems Characterization, 2015, 32, 340-346.	2.3	11
76	Surface versus Bulk Currents and Ionic Space-Charge Effects in CsPbBr ₃ Single Crystals. Journal of Physical Chemistry Letters, 2022, 13, 3824-3830.	4.6	11
77	Radiation hardness of the storage phosphor europium doped potassium chloride for radiation therapy dosimetry. Medical Physics, 2011, 38, 4681-4688.	3.0	10
78	Optimization of synthesis and compositional parameters of magnesium germanate and fluoro-germanate thermographic phosphors. Journal of Alloys and Compounds, 2018, 734, 29-35.	5.5	10
79	Discriminating bulk versus interface shunts in organic solar cells by advanced imaging techniques. Progress in Photovoltaics: Research and Applications, 2019, 27, 460-468.	8.1	10
80	Characterization of the phosphor (Sr,Ca)SiAlN3: Eu2+ for temperature sensing. Journal of Luminescence, 2020, 226, 117487.	3.1	10
81	Determination of the complex refractive index of powder phosphors. Optical Materials Express, 2017, 7, 2943.	3.0	8
82	Building process design rules for microstructure control in wide-bandgap mixed halide perovskite solar cells by a high-throughput approach. Applied Physics Letters, 2021, 118, .	3.3	8
83	Morphology-Controlled Organic Solar Cells Improved by a Nanohybrid System of Single Wall Carbon Nanotubes Sensitized by PbS Core/Perovskite Epitaxial Ligand Shell Quantum Dots. Solar Rrl, 2017, 1, 1700043.	5.8	7
84	Enhanced photosynthetic activity in Spinacia oleracea by spectral modification with a photoluminescent light converting material. Optics Express, 2013, 21, 909.	3.4	7
85	Overcoming Temperatureâ€Induced Degradation of Silver Nanowire Electrodes by an Ag@SnO _x Coreâ€Shell Approach. Advanced Electronic Materials, 2022, 8, .	5.1	7
86	Spectral hole burning in Sm2+-doped alkaliborate glasses and Tb3+-doped silicate and borate glasses. Journal of Luminescence, 2000, 86, 323-332.	3.1	6
87	Semitransparent Organic Light Emitting Diodes with Bidirectionally Controlled Emission. ACS Photonics, 2016, 3, 1233-1239.	6.6	6
88	Micropowder Ca2YMgScSi3O12:Ce Silicate Garnet as an Efficient Light Converter for White LEDs. Materials, 2022, 15, 3942.	2.9	6
89	Crystallization and Investigation of the Structural and Optical Properties of Ce3+-Doped Y3â^'xCaxAl5â^'ySiyO12 Single Crystalline Film Phosphors. Crystals, 2021, 11, 788.	2.2	5
90	Spontaneous alloying of ultrasmall non-stoichiometric Ag–In–S and Cu–In–S quantum dots in aqueous colloidal solutions. RSC Advances, 2021, 11, 21145-21152.	3.6	5

#	Article	IF	CITATIONS
91	Characterization of Aerosol Deposited Cesium Lead Tribromide Perovskite Films on Interdigited ITO Electrodes. Advanced Electronic Materials, 2021, 7, 2001165.	5.1	5
92	Photoluminescent and storage properties of photostimulable core/shell type silicate nanoparticles. Physica Status Solidi C: Current Topics in Solid State Physics, 2013, 10, 180-184.	0.8	4
93	Effect of Post-Annealing Treatment on the Structure and Luminescence Properties of AIN:Tb ³⁺ Thin Films Prepared by Radio Frequency Magnetron Sputtering. Materials Science Forum, 0, 890, 299-302.	0.3	4
94	Luminescent Properties of Nanopowder and Singleâ€Crystalline Films of TbAG:Ce Garnet. Physica Status Solidi (B): Basic Research, 2020, 257, 1900495.	1.5	4
95	Novel two-dimensional phosphor thermography by decay-time method using a low frame-rate CMOS camera. Optics and Lasers in Engineering, 2020, 128, 106010.	3.8	4
96	Highly Stable Lasing from Solutionâ€Epitaxially Grown Formamidinium‣eadâ€Bromide Microâ€Resonators. Advanced Optical Materials, 2022, 10, .	7.3	3
97	An Innovative Anode Interface Combination for Perovskite Solar Cells with Improved Efficiency, Stability, and Reproducibility. Solar Rrl, 2022, 6, .	5.8	3
98	Spectroscopic Study of Formation of Irradiation Defects in Diamond, Suitable for Persistent Spectral Hole Burning. Molecular Crystals and Liquid Crystals, 1996, 291, 241-249.	0.3	2
99	Temperature and pressure dependence of the homogeneous width of 7F0–5D0 electronic transition in Sm2+-doped sodium borate glass. Journal of Luminescence, 2007, 122-123, 74-76.	3.1	2
100	Red-emitting Ca1-xSrxS:Eu2+ Phosphors as Light Converters for Plant-growth Applications. Materials Research Society Symposia Proceedings, 2011, 1342, 15.	0.1	2
101	Luminescent down-shifting layers with Eu ²⁺ and Eu ³⁺ doped strontium compound particles for photovoltaics. Proceedings of SPIE, 2014, , .	0.8	2
102	Organic Solar Cells: Water Ingress in Encapsulated Inverted Organic Solar Cells: Correlating Infrared Imaging and Photovoltaic Performance (Adv. Energy Mater. 20/2015). Advanced Energy Materials, 2015, 5, n/a-n/a.	19.5	2
103	Computational optimization and solution-processing of thick and efficient luminescent down-shifting layers for photovoltaics. Proceedings of SPIE, 2016, , .	0.8	2
104	Luminescence properties of Yb3+-Tb3+ co-doped amorphous silicon oxycarbide thin films. Optical Materials, 2019, 92, 16-21.	3.6	2
105	Effect of water vapor content during the solid state synthesis of manganese-doped magnesium fluoro-germanate phosphor on its chemistry and photoluminescent properties. Optical Materials, 2020, 99, 109572.	3.6	2
106	A General Guideline for Vertically Resolved Imaging of Manufacturing Defects in Organic Tandem Solar Cells. Advanced Materials Interfaces, 2020, 7, 2000336.	3.7	2
107	Perspectives of solution epitaxially grown defect tolerant lead-halide-perovskites and lead-chalcogenides. Applied Physics Letters, 2021, 119, .	3.3	2
108	Memory and neural networks on the basis of color centers in solids. Biological Chemistry, 2009, 390, 1133-1138.	2.5	1

#	Article	IF	CITATIONS
109	Photostimulable Fluorescent Nanoparticles for Biological Imaging. Materials Research Society Symposia Proceedings, 2011, 1342, 21.	0.1	1
110	Rare-Earth Ion-Based Photon Up-Conversion for Transmission-Loss Reduction in Solar Cells. , 2022, , 241-267.		1
111	Preparation of luminescent inorganic core/shell-structured nanoparticles. Materials Research Society Symposia Proceedings, 2011, 1342, 3.	0.1	0
112	Quantitative Analysis of Charge Dissociation by Selectively Characterizing Exciton Splitting Efficiencies in Single Component Materials. Israel Journal of Chemistry, 0, , .	2.3	0
113	Unraveling the Charge Carrier Dynamics from the Femtosecond to the Microsecond Timescale in Double-cable Polymer-based Single-component Organic Solar Cells. , 0, , .		0